



Contents lists available at ScienceDirect

NeuroToxicology



Full Length Article

Cellular responses of human astrocytoma cells to dust from the Acheson process: An *in vitro* study

Yke Jildouw Arnoldussen^a, Torunn Kringlen Ervik^a, Balazs Berlinger^a, Ida Kero^b, Sergey Shaposhnikov^c, Shanbeh Zienolddiny^{a,*}

^a Department of Biological and Chemical Work Environment, National Institute of Occupational Health, Pb 8149 Dep., N-0033, Oslo, Norway

^b Department of Industrial Process, Technology SINTEF Materials and Chemistry, PB 4760, N-7465, Trondheim, Norway

^c Norgenotech AS & Comet Biotech AS, N-1290 Oslo, Norway

ARTICLE INFO

Article history:

Received 8 August 2017

Received in revised form 2 November 2017

Accepted 2 November 2017

Available online xxx

Keywords:

Acheson process

Neurotoxicity

Astrocytes

Silicon carbide

ABSTRACT

Silicon carbide (SiC) is largely used in various products such as diesel particulate filters and solar panels. It is produced through the Acheson process where aerosolized fractions of SiC and other by-products are generated in the work environment and may potentially affect the workers' health. In this study, dust was collected directly on a filter in a furnace hall over a time period of 24 h. The collected dust was characterized by scanning electron microscopy and found to contain a high content of graphite particles, and carbon and silicon containing particles. Only 6% was classified as SiC, whereof only 10% had a fibrous structure. To study effects of exposure beyond the respiratory system, neurotoxic effects on human astrocytic cells, were investigated. Both low, occupationally relevant, and high doses from 9E-6 $\mu\text{g}/\text{cm}^2$ up to 4.5 $\mu\text{g}/\text{cm}^2$ were used, respectively. Cytotoxicity assay indicated no effects of low doses but an effect of the higher doses after 24 h. Furthermore, investigation of intracellular reactive oxygen species (ROS) indicated no effects with low doses, whereas a higher dose of 0.9 $\mu\text{g}/\text{cm}^2$ induced a significant increase in ROS and DNA damage. In summary, low doses of dust from the Acheson process may exert no or little toxic effects, at least experimentally in the laboratory on human astrocytes. However, higher doses have implications and are likely a result of the complex composition of the dust.

© 2017 The Author(s). Published by Elsevier B.V. This is an open access article under the CC BY-NC-ND license (<http://creativecommons.org/licenses/by-nc-nd/4.0/>).

1. Introduction

Silicon carbide (SiC) produced by the Acheson process is a well-known ceramic material known for its properties such as chemical inertness, elevated thermal stability and excellent mechanical properties. It is used in a wide variety of industrial purposes both in the ceramic and composite material fields (Oliveros et al., 2013). Furthermore, there is an increased interest in the use of micro and nanoscale SiC materials in the areas of ceramics, electronics and catalysis. Thus, as SiC likely will continue to be used in a various number of products, research on potential health effects due to occupational exposure will be of importance.

Most toxicological effects related to SiC from the Acheson process have focused on the respiratory effects and most of the knowledge is on SiC whiskers. Analyses on the effects of dust exposure of workers in the SiC industry have indicated increased loss of lung function, increased mortality from non-malignant

respiratory diseases and increased incidence of lung cancer (Bugge et al., 2011, 2012; Johnsen et al., 2013). Due to their ability to cause lung cancer, occupational exposure associated with the Acheson process has been classified as carcinogenic to humans by the International Agency for Research on Cancer (Grosse et al., 2014).

Subchronic inhalation and intrapleural injection of SiC whiskers in rats induced inflammatory lesions, thickening of the pleural wall, pleural fibrosis and mesotheliomas (Lapin et al., 1991; Johnson and Hahn, 1996). Studies on SiC microparticles showed that the particles triggered lung inflammation (Cullen et al., 1997), granulomas (Vaughan et al., 1993), fibrotic changes in the lungs (Akiyama et al., 2007), exerted cytotoxic and genotoxic effects (Vaughan et al., 1993), induced reactive oxygen species (ROS) (Svensson et al., 1997) and increased the expression of inflammatory cytokines (Cullen et al., 1997). Furthermore, accumulation of nanoscale SiC particles was observed in lung epithelial cells and induced ROS and DNA damage (Fan et al., 2008; Barillet et al., 2010).

There is little knowledge on potential neurotoxic effects of dust from the Acheson process. Dust emitted from the Acheson process has several components, including silica particles that may have an

* Corresponding author.

E-mail address: shan.zienolddiny@stami.no (S. Zienolddiny).

<https://doi.org/10.1016/j.neuro.2017.11.001>

0161-813X/© 2017 The Author(s). Published by Elsevier B.V. This is an open access article under the CC BY-NC-ND license (<http://creativecommons.org/licenses/by-nc-nd/4.0/>).

impact on the central nervous system. Nanoscale silica particles showed increased oxidative damage and inflammatory responses in the brain after intranasal instillation in experimental animals (Wu et al., 2011). Furthermore, uptake of silica nanoparticles decreased neuron cell viability, induced ROS, apoptosis, and increased Alzheimer-like pathology (Yang et al., 2014). Supporting this, a recent study showed that silica nanoparticles can cross the blood-brain barrier and induce neuronal cell damage (Zhou et al., 2016). Other elements, such as carbon, aluminum and vanadium, that can be part of occupational exposure in the Acheson furnace hall have all been shown to have neurotoxic effects (Campbell, 2002; Garcia et al., 2005; Onoda et al., 2017).

We sought to investigate the effects of dust collected in the furnace hall of a SiC facility on a human astrocytic cell line cultured in the laboratory. The human cells were exposed to a range of doses, including low occupationally relevant, and high doses. The results showed minimal dose-dependent toxicity, ROS production and DNA damage.

2. Materials and methods

2.1. Collection of the Acheson dust

A 142 mm stainless steel filter holder, YY3014236 (Merck Millipore, Massachusetts, USA) was placed in the middle of an Acheson furnace hall close to one of the furnaces. A 142 mm diameter polycarbonate filter with pore size 10 µm was placed on top of the filter holder and then connected to a high output vacuum pump, WP6222050 (Merck Millipore, Massachusetts, USA), with adjustable output. This was left on for a period of 24 h where dust was collected from the filter three times during this period. The dust can be considered as an impure powder with no industrial application and is representative of the airborne dust that can be inhaled in the work environment of a furnace hall.

2.2. Preparation of the Acheson dust for characterization and cell culture experiments

The dust was weighed and for dispersion a slightly modified version of the NANOGENOTOX protocol was used (Jensen et al., 2011; Phuyal et al., 2017). Briefly, to obtain well-dispersed particles a solution of sterile-filtered 0.05% Bovine Serum Albumin (BSA) (diluted in H₂O, m/v) was added to obtain a stock solution of 1 mg/ml. After a brief vortexing, the solution was sonicated using a probe sonicator at 10% amplitude (Sonifier 450S, Branson Ultrasonics, Danbury, USA) for 15 min. For each single experiment a freshly prepared stock was used. In the cell culture experiments, controls were exposed to the highest volume of 0.05% BSA that was used to prepare the highest dose of Acheson dust for exposure. For the highest dose of Acheson dust (4.5 µg/cm²) this corresponded to a final BSA concentration of 0.000675% in the cell culture media.

2.3. Acheson dust characterization

2.3.1. SEM

The Acheson dust was prepared as follows: a volume corresponding to 100 µg was taken from a 1 mg/ml stock dispersed in 0.05% BSA which was sonicated as described above followed by filtering on a 47 mm Whatman Nuclepore polycarbonate filter with 50 nm pore size. Thereafter the filter was coated with a thin platinum film in a sputter coater (Cressington 208HR sputter coater, UK). Specimens of 10 × 10 mm were cut from the filter and gently fixed on aluminum specimen stubs with double-sided

carbon adhesive discs. The specimens were analyzed with a Hitachi SU 6600 (Ibaraki-ken, Japan) field emission scanning electron microscope (FE-SEM) equipped with a Bruker energy-dispersive X-ray detector. The instrument was operated under the following conditions: accelerating voltage 15 keV and working distance 10 mm. High resolution images of the particles were obtained by acquiring at slow scanning speed. Initially, specimens were examined in the SEM to determine their morphology and size. The chemical composition of the Acheson dust particles was obtained by energy dispersive x-ray spectroscopy (EDX).

2.3.2. Dynamic light scattering

To obtain information on the dusts' hydrodynamic size distribution after dispersion, ZetaSizer Nano ZS (Malvern Instruments Ltd, UK) was used. Immediately after sonication 1 ml of the sonicated solution was pipetted into a cuvette, left on the bench for 5 min and was thereafter left for 5 min in the ZetaSizer apparatus before measuring over 10 cycles. ZetaSizer software (Malvern Instruments Ltd, UK) was used to analyze the data. The results shown are from three independent measurements.

2.4. Cells and cell culture

The human astrocytoma 1321N1 cell line was purchased from Sigma-Aldrich (catalogue no. 86030402). These are glial cells from a human brain astrocytoma that was initially isolated in 1972 as a sub clone of the cell line 1181N1 (Macintyre et al., 1972). Cells were routinely kept in a humidified 5% CO₂ and 95% air incubator at 37 °C in Dulbecco's Modified Eagle's Medium (DMEM, Fisher Scientific) containing 10% fetal bovine serum (FBS, Biochrom), 50 U/ml penicillin and 50 µg/ml streptomycin (Thermo Scientific). The passage number of the cells was kept below 30.

2.5. Estimation of dust doses used for cell culture experiments

The doses used for cell culture exposures were kept low to mimic occupational exposure and were calculated following a mathematical calculation modified from Antonini and coworkers (Antonini et al., 2010, 2013) to determine the daily lung burden of a worker working 8 h per day. Incorporated factors were the occupational exposure limit for respirable dust in the silicon carbide industry (0.5 mg/m³), human minute ventilation volume (20,000 ml/min × E-6 m³/ml), the exposure duration (8 h/day), the deposition efficiency (set to 20%; (Oberdorster et al., 2005a, 2005b)).

The daily deposited dose was:

$$0.5 \text{ mg/m}^3 \times (20,000 \text{ ml/min} \times 10^{-6} \text{ m}^3/\text{ml}) \times (8 \text{ h} \times 60 \text{ min/h}) \times 0.20 = 0.96 \text{ mg}$$

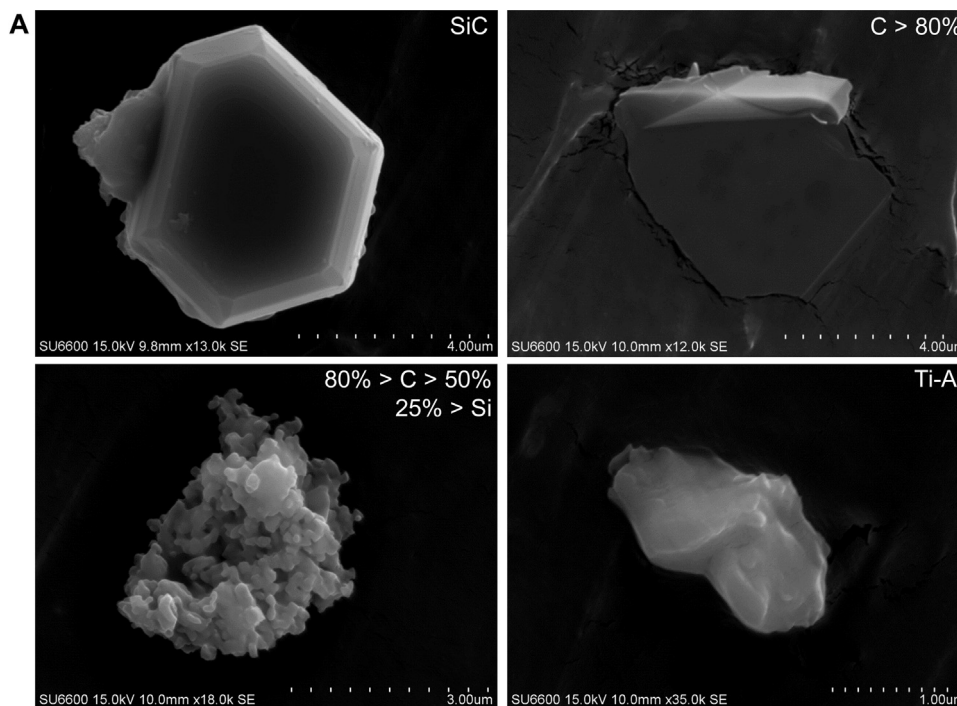
When using the surface area of the alveolar epithelium (human 102 m² (Stone et al., 1992)) this leads to a deposited dose of 9E-4 µg/cm² (0.96 mg/1,020,000 cm² = 0.9E-6 mg/cm² → 0.0009 µg/cm²). This dose was set as 1x and the other doses (0x, 0.01x, 0.1x, 10x, 100x, 1000x, 5000x) used in this study were calculated accordingly. Thus cells were exposed to 0, 9E-6, 9E-5, 9E-4, 9E-3, 0.09, 0.9 and 4.5 µg/cm² taking into account the surface area of the cell culture dish, respectively.

2.6. Cytotoxicity assay

For each toxicity experiment 5000 cells/well were seeded in triplicate in black 96-well plates with a transparent bottom (Nunclon, Thermo Scientific). Cells were allowed to attach for 24 h prior to addition of dispersed Acheson dust at the indicated doses.

Thereafter the medium was removed and the cells were washed once with phosphate-buffered saline (PBS) to remove excess particles. The Cell Counting Kit-8 (CCK-8) assay (Sigma-Aldrich) was used to measure cytotoxicity levels by diluting it in the cell culture media without supplements according to the manufacturer’s instructions.

After incubation at 37 °C for 1 h, absorbance as optical density (OD) was measured at 450 nm using a SpectraMax i3 (Molecular Devices, California, USA). In addition, OD was measured at 750 nm as a reference wavelength for background detection and was subtracted



B Characteristics	Number (%) n = 308	Morphology
SiC	6	
C > 80%	34	
80% > C > 50% 25% > Si	29	
Ti – Al	22	
Ti – Al – V	8	

Acheson dust	Z-average (nm) ± stdev		
	Peak 1	Peak 2	Peak 3
	426 ± 57	144 ± 30	5374 ± 78

Fig. 1. Characterization of the collected Acheson dust. A) A volume corresponding to 100 µg dust was taken from a 1 mg/ml stock dispersed in 0.05% BSA and filtered through a 47 mm Whatman Nuclepore polycarbonate filter with 50 nm pore size. The dust was investigated by SEM and representative images were taken from the different particles that were found. Representative images of particles containing SiC, C > 80%, 80% > C > 50% and 25% > Si, Ti-Al are shown. B) Particles were divided into groups according to their morphology and elemental contents. Percentages and representative SEM images of each particle type are shown. n = 308. SiC: silicon carbide, C: carbon, Si: silicon, Ti: titanium, Al: aluminum. C) Overview of particle size measured by dynamic light scattering. After sonication of the Acheson dust 1 ml of solution (1 mg/ml) was immediately transferred to a transposable cuvette and left on the bench for 5 min and thereafter inside the machine for 5 min before measuring. 10 cycles were run. The Z-average from three independent dispersed batches is shown ± standard deviation (SD).

from sample OD at 450 nm. A standard curve with a known number of cells was established to calculate the number of cells in each well.

2.7. Measurement of intracellular ROS

Intracellular ROS levels were measured using dichlorodihydrofluorescein (DCF) fluorescence. 2',7'-dichlorodihydrofluorescein diacetate (DCFH/DA) (Sigma-Aldrich) is a cell-permeable compound that yields a fluorescent product when oxidized by ROS. 1321N1 cells were seeded in sixwell plates, allowed to attach for two days and exposed to the dispersed Acheson dust for 24, 48 and 72 h. The protocol for ROS measurement is modified from (Li and Ellis, 2014). Briefly, following exposure the medium was removed and medium containing 100 μ M DCFH/DA was added to the cells which were then incubated at 37 °C for 1 h. Positive and negative controls were included in each experiment. Cells were then washed with 1 x PBS and incubated with 2% TritonX-100 in PBS on ice for 5 min. Cells were collected in Eppendorf tubes by scraping and then sonicated on a VialTweeter (UIS250 V, Hielscher Ultrasonics GmbH, Teltow, Germany) for 2 x 5 s at maximum amplitude. Thereafter tubes were centrifuged at 15,000 RPM for 10 min at 4 °C and supernatant was transferred to new Eppendorf tubes. Each sample was added in triplicate to a 96-well plate and fluorescence was measured using SpectraMax i3 (Molecular Devices, California, USA) upon excitation of 488 nm. Finally, the protein concentration of each sample was measured and DCF fluorescence was calculated relative to the protein content of each sample.

2.8. Assessment of DNA damage with the comet assay

To examine DNA damaging effects after Acheson dust exposure, the modified comet assay was performed following a previously described protocol (Azqueta et al., 2014). Briefly, cells were seeded on sixwell Plates 24 h before exposure. Cells were then exposed to the Acheson dust for 24, 48 and 72 h. At the end of exposure, cells were harvested by trypsinization, mixed with low melting point (LMP) agarose and two drops from this mixture were placed on glass slides that were pre-coated with 0.5% standard melting point agarose. After lysis in cold lysis buffer (2.5 M NaCl, 0.1 M EDTA, 10 mM Tris, 1% Triton X-100, pH10), incubation in cold 0.3 M NaOH, 1 mM EDTA for 20 min and electrophoresis in the same buffer at 0.8 V/cm for 20 min, slides were neutralized with PBS and stained with SybrGold[®] (Invitrogen) diluted in TE buffer. Slides were then examined under a Nikon fluorescent microscope using Comet assay IV software (Perceptive Instruments, UK), where mean% DNA in comet tails from 100 comets/gel was used as a measure of DNA

strand breaks. To detect oxidative DNA damage, post-lysis incubation with the formamidopyrimidine DNA glycosylase (Fpg) was also carried out. Fpg is a multifunctional DNA base excision repair enzyme that removes a wide range of oxidatively-damaged bases (N-glycosylase activity) creating a so called apurinic/aprimidinic site (AP site); and its AP lyase activity cleaves both the 3'- and 5'-phosphodiester bonds of the resulting AP site. The AP lyase activity introduces nicks in the DNA strand, cleaving the DNA backbone to generate a single-strand break at the site of the removed base with both 3'- and 5'-phosphates. Fpg has a preference for oxidized purines, excising oxidized purines such as 7,8-dihydro-8-oxoguanine (8-oxoG). Since Fpg converts oxidized purines to strand breaks, this allows indirect readout of oxidative base lesions.

2.9. Statistics

Statistical analyses were performed in SigmaPlot (Systat, USA). The data were analyzed using one way ANOVA followed by Tukey's post hoc test. In case of lack of normal distribution the Kruskal-Wallis test followed by Tukey's post hoc test was used. Statistical significance was assessed at $P < 0.05$.

3. Results

3.1. Characteristics of the Acheson dust

The dust collected in the furnace hall of a SiC factory was characterized by scanning electron microscopy (SEM) and energy dispersive x-ray spectroscopy (EDX). Representative images of some of the particle structures are shown in Fig. 1A. The total number of particles investigated ($n = 308$) were divided into groups taking into account their morphology and elemental content (Fig. 1B). The largest group (34%) of particles were characterized by a high percentage of carbon (>80% C) and flake-like morphology. The next particle group represents 29% of the total number of particles examined and had a carbon content between 50 and 80%, combined with a silicon content below 25%, in addition to oxygen. These particles had different structures, including droplet-like and more irregularly shaped particles. As seen from Fig. 1A, the particles appear to be agglomerates of smaller particles which may explain the somewhat large variations in carbon and silicon content. The agglomerates may consist of smaller SiC particles. The interaction volume of x-rays is large and generates EDX signal from an effective volume much larger than the actual particle investigated and quantitative EDX analysis is therefore difficult. Furthermore, 22% of the examined particles contained titanium

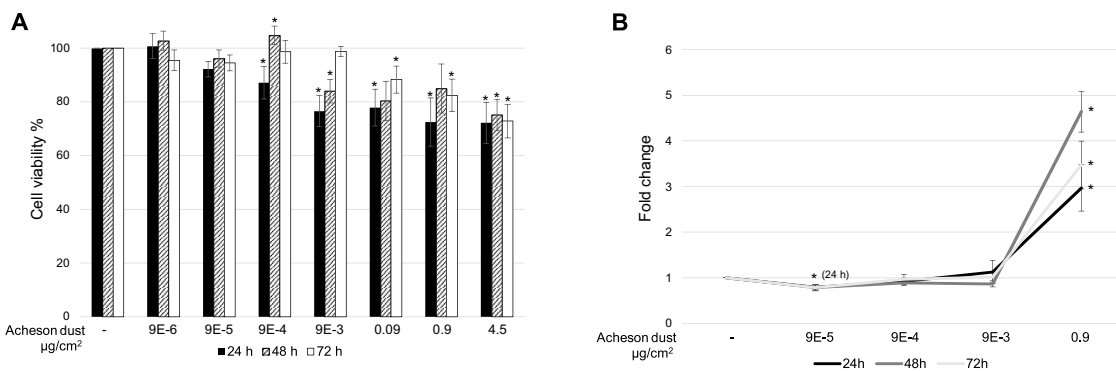


Fig. 2. Acheson dust-induced cytotoxicity and ROS are dose- and time-dependent. A) Human 1321N1 astrocytoma cells were grown and exposed to sham or to Acheson dust at the indicated concentrations for 24, 48 and 72 h before measurement of cellular cytotoxicity. Cell viability of sham-treated cells was set to 100%. B) The indicated doses were used to measure the levels of intracellular ROS after 24, 48 and 72 h. Sham-treated controls were set to 1 and the mean fold change from three independent experiments in triplicate is shown. Bars: SE. *: $P < 0.05$ indicates a significant difference between exposed cells and the corresponding sham-treated control.

(~25% Ti) and aluminum (~2.7% Al), and 8% of the particles contained titanium (~38% Ti), aluminum (~3% Al) and vanadium (~2.7% V). At the site of collection, the airborne particulate matter seem to have come from raw materials and sources unrelated to the active furnace heat zone. The small fraction of SiC may be attributed to the fact that no furnaces were being dismantled in the proximity of the sampling equipment during sampling. Moreover, only two of the 308 (approx. 0.65%) investigated particles had a fibrous shape. Measurements of the hydrodynamic size by dynamic light scattering indicated that the majority of the particles had a Z-average of 426 ± 57 nm followed by a peak of 144 ± 30 nm that are higher than the suggested 100 nm to be considered nanoscale particles (Fig. 1C). These sizes correspond to the sizes of the smallest particles, including titanium and aluminum (22%) and titanium, aluminum and vanadium containing particles (8%) found by SEM. In addition, a peak of 5374 ± 78 nm was detected and likely consists of the larger SiC-, carbon- and silicon-containing particles.

3.2. The effect of Acheson dust on cell viability, ROS generation and DNA damage

Exposure of the cells to the increasing concentrations of Acheson dust indicated a dose-dependent effect on cell viability which was reversible at later time points (Fig. 2A). All doses except for 9E-6 and 9E-5 $\mu\text{g}/\text{cm}^2$ induced a significant reduction in cell viability after 24 h. For both 9E-4 and 9E-3 $\mu\text{g}/\text{cm}^2$ this response was biphasic as cell viability increased. After 72 h the highest and not occupational relevant doses of 0.09, 0.9 and 4.5 $\mu\text{g}/\text{cm}^2$ had a significant impact on the cell viability. Thus, the cytotoxic effect of the Acheson dust on the 1321N1 cells is dose-dependent but transient where the initial reduction in cell viability observed after 24 h is reversible after 48 and 72 h with low occupational relevant doses (Fig. 2A). Four doses, including 9E-5, 9E-4, 9E-3 and 0.9 $\mu\text{g}/\text{cm}^2$ were chosen for further experiments. The low doses would be comparable of occupational exposure scenarios, whereas the higher doses were included to look for extreme and overload exposure scenarios.

Investigation of the levels of intracellular ROS showed that the low doses up to 9E-3 $\mu\text{g}/\text{cm}^2$ did not induce ROS (Fig. 2B). Moreover, a significant reduction was observed for the 9E-5 $\mu\text{g}/\text{cm}^2$ dose after 24 h. The highest dose, 0.9 $\mu\text{g}/\text{cm}^2$, gave a significant increase in ROS levels at all the time points tested and peaked at 48 h. Thus, low and occupationally more relevant doses of the Acheson dust do not induce ROS.

To further investigate the molecular effects of the Acheson dust on the 1321N1 cells, comet assay was performed to detect possible damage to the DNA. The results showed an increase in DNA damage after 24 h which was significant for the highest dose, 0.9 $\mu\text{g}/\text{cm}^2$ (Fig. 3A). This response was reversible as no changes were observed after 48 and 72 h, except for a significant decrease in DNA damage for the 0.9 $\mu\text{g}/\text{cm}^2$ dose after 48 h. Furthermore, a significant, although small, increase was shown with 9E-4 and 9E-3 $\mu\text{g}/\text{cm}^2$ after 72 h. To investigate possible oxidative DNA damage following exposure to Acheson dust, post-lysis incubation with Fpg was also performed. The indirect readout of oxidative base lesions showed that there were no significant changes for all the doses and time points tested (Fig. 3B).

4. Discussion

Exposure to emitted dust in industrial processes poses a potential human health problem. There may be a correlation between health effects and exposures to known air contaminants in SiC plants. Little research has been performed on the effects of dust collected directly from the furnace hall in the SiC industry on

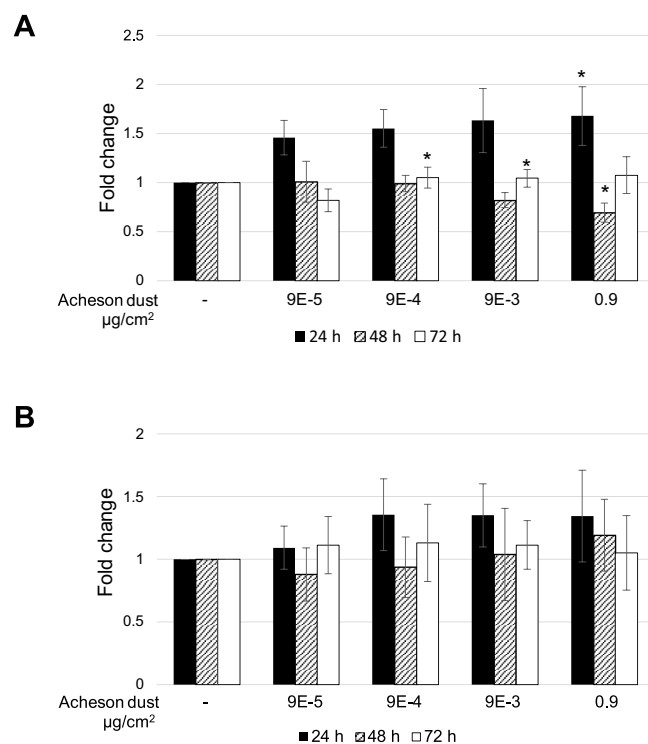


Fig. 3. DNA damage in the 1321N1 astrocytoma cells after exposure to the Acheson dust. A) Cells were exposed to the indicated doses of Acheson dust for the indicated times. Thereafter damage to the DNA was investigated using the comet assay as described in Materials and Methods. For analysis the percentage of tail intensity was calculated. B) Oxidative damage to the DNA was also investigated by post-lysis incubation with Fpg. For analysis the percentage of tail intensity was calculated. Fold change for each exposure from three independent experiments in triplicate is shown with sham-treated controls set to 1. Bars: SE. *: $P < 0.05$ indicates a significant difference between exposed cells and the corresponding sham-treated control.

human brain cells. However, in other cell types such as RAW264.7 macrophages that were exposed to various manufactured SiC powders collected from the Acheson process and to a SiC powder representative of airborne dust this did not induce cytotoxicity in doses ranging from 20 to 120 $\mu\text{g}/10^6$ cells after 24 h (Boudard et al., 2014). However, the airborne dust representative induced tumor necrosis factor α (TNF α) possibly due to the presence of crystalline silica and iron impurities (Boudard et al., 2014).

Toxicity of particles is closely related to their physico-chemical properties, including size, shape, surface area, and chemical composition. The raw materials for SiC production consist of quartz sand and petroleum coke, in addition to both unreacted and partly reacted material from previous furnace cycles. Graphite is used as an electric conductor and therefore traces of graphite may also be present. Most concern on dust from the Acheson process is on SiC fibers and most studies focus on this. In our collected material only ~6% consisted of SiC and among the particles detected as SiC, only 10% had a fibrous structure. Other studies from both Norway and Canada have reported on airborne fibers and presence of carbonaceous matter, quartz, cristobalite, SiC, respirable dust, benzene soluble matter and common polycyclic aromatic hydrocarbons (Bye et al., 1985; Dufresne et al., 1987, 1995; Dion et al., 2005). As the furnace hall contains a mixture of dusts and gases the exposure pattern may be different at various places in the furnace hall. Moreover, the levels of impurities will likely be different for the various Acheson process workplaces where dust is collected. These factors would complicate comparison of different studies.

The doses in the present study were kept very low to mimic occupational exposure scenarios and were estimated taking into consideration the occupational exposure situations for particulate matter from the Acheson process. The Acheson dust had a dose- and time-dependent effect on the cells. With the lowest doses the initial decrease in cell viability as a response to acute toxicity was biphasic as cell viability was restored at later time points. The highest dose, 0.9 $\mu\text{g}/\text{cm}^2$, induced a significant increase in ROS and corresponded to a continuing decrease in cell viability. Thus, for the lower doses detoxification processes might have restored cell viability probably due to increased cell proliferation, whereas this was not obtained for the higher doses. It is known that particle-induced ROS can occur in various ways, including the presence of pro-oxidant groups on the surface of the particles, redox reactions on the surface of metals and particle-cell interactions (Manke et al., 2013). Furthermore, as the induction of ROS was transient with 0.9 $\mu\text{g}/\text{cm}^2$, peaking after 48 h, this may indicate activation of detoxification processes to reduce these levels. Transient increases in ROS levels have also been reported by others (Barillet et al., 2010; Manke et al., 2013; Carrasco et al., 2016). However, at this time cell viability was not completely restored and indicates that other cellular processes are activated that contribute to the reduced cell viability. As there were small and transient effects on cell viability and ROS production it was of interest to investigate possible damage to the DNA. Also, ROS levels may increase due to damage to the DNA (Rowe et al., 2008; Kang et al., 2012) and has been shown to be important for the regulation of cell survival and apoptosis (Simon et al., 2000; Hamanaka and Chandel, 2010). The data indicated DNA damage after 24 h with the highest dose tested, and after 72 h with 9E-4 and 9E-3 $\mu\text{g}/\text{cm}^2$. However, the levels are very low and for the highest dose reversible, indicating that DNA repair mechanisms possibly are activated. Furthermore, testing for oxidative damage by including Fpg in the assay indicated no significant differences, but other types of DNA damage cannot be ruled out.

Exactly what fraction of the Acheson dust that causes the increase in cytotoxicity, ROS and DNA damage is not known. Metal impurities have an impact on these endpoints and the Acheson dust used here contains a variety of elements that may cause the observed effects. Several studies have investigated the effects of different types of particles on primary astrocytes. A study focusing on carbon showed that astrocytes grown on carbon decreased their function (Mckenzie et al., 2004). Work performed on carbon black nanoparticles showed that mice exposed to this material induced a long-term activation of astrocytes resulting in reactive astrogliosis in the brains of their offspring, probably due to the presence of carbon (Onoda et al., 2017). Moreover, several neurotoxicological studies have been performed on the effects of aluminum exposure. It has been associated with a variety of neurological disorders linked to an increase in oxidative and inflammatory events leading to tissue damage (Campbell, 2002). Cultured astrocytes exposed to aluminum had an intracellular accumulation and reduced cell viability was characterized by DNA fragmentation and apoptosis (Suarez-Fernandez et al., 1999). Vanadium, another element present in the dust, has previously been shown to be neurotoxic to the central nervous system in rats where it increased the presence of enlarged astrocytes in the cerebellum and hippocampus (Garcia et al., 2005). As most studies on dust from the SiC industry mainly focus on SiC, in particular SiC fibers, one must not forget the possible effects caused by other elemental contents.

In the current study, an astrocytoma cell line was employed. The 1321N1 cell line is well-established and used in many studies investigating neurotoxic effects of various compounds, and could be a suitable cell model to gain insight in possible effects after exposure to Acheson dust. However, the characteristics of these cells may differ from primary cells and therefore, a similar study

using primary astrocytes would be more relevant. During the experiments serum was used in the cell culture media as recommended by the manufacturer. As serum may vary from batch to batch this may have had a small potential impact on the results. The occupationally relevant doses we have used in this study do not reflect the actual amount of particles that are translocated into the circulation through uptake by the blood in the lungs or by the olfactory bulb. Differences in breathing, deposition in upper airways, and clearance of the particles from the airways and particle characteristics will influence the actual deposition in the alveolar region. Studies on the actual amount of particles passing from the lungs to the blood are few and inconclusive. A study by Geiser and Kreyling showed for example that a very low percentage may translocate from lungs and cross the blood brain barrier and enter the brain (Geiser and Kreyling, 2010). Therefore, the doses used in the present study would still be high compared to the dose that may ultimately enter the brain after occupational exposure.

Conclusively, the main idea of this study was to look for cytotoxic effects of dust from the Acheson process, and then to look if the toxicity could be related to increased ROS production followed by if ROS production was due to damage to DNA bases, specifically purines, or whether it was not related to DNA damage. At this point, our mechanistic data suggest that the Acheson dust may not be highly toxic at least at low doses or there might be a transient toxicity which may not be related to permanent damage to DNA bases.

Conflict of interest

None of the authors has any potential conflict of interest or financial interests to disclose.

Acknowledgements

This work was supported by a postdoctoral grant from the Research Council of Norway to YJA (RCN grant no. 245216 070). We would like to thank Vaineta Vebrate for excellent help with the comet assays.

References

- Akiyama, I., Ogami, A., Oyabu, T., Yamato, H., Morimoto, Y., Tanaka, I., 2007. Pulmonary effects and biopersistence of deposited silicon carbide whisker after 1-year inhalation in rats. *Inhal. Toxicol.* 19, 141–147.
- Antonini, J.M., Roberts, J.R., Chapman, R.S., Soukup, J.M., Ghio, A.J., Sriram, K., 2010. Pulmonary toxicity and extrapulmonary tissue distribution of metals after repeated exposure to different welding fumes. *Inhal. Toxicol.* 22, 805–816.
- Antonini, J.M., Roberts, J.R., Schwegler-Berry, D., Mercer, R.R., 2013. Comparative microscopic study of human and rat lungs after overexposure to welding fume. *Ann. Occup. Hyg.* 57, 1167–1179.
- Azqueta, A., Slyskova, J., Langie, S.A., Gaivau, I.O'Neill, Collins, A., 2014. Comet assay to measure DNA repair: approach and applications. *Front. Genet.* 5, 288.
- Barillet, S., Jugan, M.L., Laye, M., Leconte, Y., Herlin-Boime, N., Reynaud, C., Carriere, M., 2010. In vitro evaluation of SiC nanoparticles impact on A549 pulmonary cells: cyto- genotoxicity and oxidative stress. *Toxicol. Lett.* 198, 324–330.
- Boudard, D., Forest, V., Pourchez, J., Boumahdi, N., Tomatis, M., Fubini, B., Guillhot, B., Cottier, M., Grosseau, P., 2014. In vitro cellular responses to silicon carbide particles manufactured through the Acheson process: impact of physico-chemical features on pro-inflammatory and pro-oxidative effects. *Toxicol. In Vitro* 28, 856–865.
- Bugge, M.D., Foreland, S., Kjaerheim, K., Eduard, W., Martinsen, J.I., Kjuus, H., 2011. Mortality from non-malignant respiratory diseases among workers in the Norwegian silicon carbide industry: associations with dust exposure. *Occup. Environ. Med.* 68, 863–869.
- Bugge, M.D., Kjaerheim, K., Foreland, S., Eduard, W., Kjuus, H., 2012. Lung cancer incidence among Norwegian silicon carbide industry workers: associations with particulate exposure factors. *Occup. Environ. Med.* 69, 527–533.
- Bye, E., Eduard, W., Gjonnes, J., Sorbroden, E., 1985. Occurrence of airborne silicon carbide fibers during industrial production of silicon carbide. *Scand. J. Work. Environ. Health* 11, 111–115.
- Campbell, A., 2002. The potential role of aluminium in Alzheimer's disease. *Nephrol. Dial. Transplant.* 17 (Suppl. 2), 17–20.

- Carrasco, E., Blázquez-Castro, A., Calvo, M.I., Juarranz, Á., Espada, J., 2016. Switching on a transient endogenous ROS production in mammalian cells and tissues. *Methods* 109, 180–189.
- Cullen, R.T., Miller, B.G., Davis, J.M., Brown, D.M., Donaldson, K., 1997. Short-term inhalation and in vitro tests as predictors of fiber pathogenicity. *Environ. Health Perspect.* 105 (Suppl. 5), 1235–12340.
- Dion, C., Dufresne, A., Jacob, M., Perrault, G., 2005. Assessment of exposure to quartz: cristobalite and silicon carbide fibres (whiskers) in a silicon carbide plant. *Ann. Occup. Hyg.* 49, 335–343.
- Dufresne, A., Lesage, J., Perrault, G., 1987. Evaluation of occupational exposure to mixed dusts and polycyclic aromatic hydrocarbons in silicon carbide plants. *Am. Ind. Hyg. Assoc. J.* 48, 160–166.
- Dufresne, A., Looserevanich, P., Armstrong, B., Infante-Rivard, C., Perrault, G., Dion, C., Masse, S., Begin, R., 1995. Pulmonary retention of ceramic fibers in silicon carbide (SiC) workers. *Am. Ind. Hyg. Assoc. J.* 56, 490–498.
- Fan, J., Li, H., Jiang, J., So, L.K., Lam, Y.W., Chu, P.K., 2008. 3C-SiC nanocrystals as fluorescent biological labels. *Small* 4, 1058–1062.
- García, G.B., Biancardi, M.E., Quiroga, A.D., 2005. Vanadium (V)-induced neurotoxicity in the rat central nervous system: a histo-immunohistochemical study. *Drug Chem. Toxicol.* 28, 329–344.
- Geiser, M., Kreyling, W.G., 2010. Deposition and biokinetics of inhaled nanoparticles. *Part. Fibre Toxicol.* 7, 2.
- Grosse, Y., Loomis, D., Guyton, K.Z., Lauby-Secretan, B., El Ghissassi, F., Bouvard, V., Benbrahim-Tallaa, L., Guha, N., Scocciati, C., Mattock, H., Straif, K., 2014. Carcinogenicity of fluoro-edenite, silicon carbide fibres and whiskers, and carbon nanotubes. *Lancet Oncol* 15, 1427–1428.
- Hamanaka, R.B., Chandel, N.S., 2010. Mitochondrial reactive oxygen species regulate cellular signaling and dictate biological outcomes. *Trends Biochem. Sci.* 35, 505–513.
- Jensen, K., Kembouche, Y., Christiansen, E., Jacobsen, N., Wallin, H., Guiot, C., 2011. 2011. The generic NANOGENOTOX dispersion protocol. *Stand. Oper. Proced. Backgr. Doc. Final Protoc. Prod. Suitable Manuf. Nanomater. Expo. Media Available* .
- Johnsen, H.L., Bugge, M.D., Foreland, S., Kjuus, H., Kongerud, J., Soyseth, V., 2013. Dust exposure is associated with increased lung function loss among workers in the Norwegian silicon carbide industry. *Occup. Environ. Med.* 70, 803–809.
- Johnson, N.F., Hahn, F.F., 1996. Induction of mesothelioma after intrapleural inoculation of F344 rats with silicon carbide whiskers or continuous ceramic filaments. *Occup. Environ. Med.* 53, 813–816.
- Kang, M.A., So, E.Y., Simons, A.L., Spitz, D.R., Ouchi, T., 2012. DNA damage induces reactive oxygen species generation through the H2AX-Nox1/Rac1 pathway. *Cell. Death. Dis.* 3, e249.
- Lapin, C.A., Craig, D.K., Valerio, M.G., Mccandless, J.B., Bogoroch, R., 1991. A subchronic inhalation toxicity study in rats exposed to silicon carbide whiskers. *Fundam. Appl. Toxicol.* 16, 128–146.
- Li, D., Ellis, E.M., 2014. Aldo-keto reductase 7A5 (AKR7A5) attenuates oxidative stress and reactive aldehyde toxicity in V79-4 cells. *Toxicol. In Vitro* 28, 707–714.
- Macintyre, E.H., Ponten, J., Vatter, A.E., 1972. The ultrastructure of human and murine astrocytes and of human fibroblasts in culture. *Acta Pathol. Microbiol. Scand. A* 80, 267–283.
- Manke, A., Wang, L., Rojanasakul, Y., 2013. Mechanisms of nanoparticle-induced oxidative stress and toxicity. *Biomed. Res. Int.* 2013, 942916.
- Mckenzie, J.L., Waid, M.C., Shi, R., Webster, T.J., 2004. Decreased functions of astrocytes on carbon nanofiber materials. *Biomaterials* 25, 1309–1317.
- Oberdorster, G., Maynard, A., Donaldson, K., Castranova, V., Fitzpatrick, J., Ausman, K., Carter, J., Karn, B., Kreyling, W., Lai, D., Olin, S., Monteiro-Riviere, N., Warheit, D., Yang, H., 2005a. A report from the ILSI Research Foundation/Risk Science Institute Nanomaterial Toxicity Screening Working Group. Principles for characterizing the potential human health effects from exposure to nanomaterials: elements of a screening strategy. *Part. Fibre Toxicol.* 2, 8.
- Oberdorster, G., Oberdorster, E., Oberdorster, J., 2005b. Nanotoxicology: an emerging discipline evolving from studies of ultrafine particles. *Environ. Health Perspect.* 113, 823–839.
- Oliveros, A., Guiseppi-Elie, A., Sadow, S.E., 2013. Silicon carbide: a versatile material for biosensor applications. *Biomed Microdevices* 15, 353–368.
- Onoda, A., Takeda, K., Umezawa, M., 2017. Dose-dependent induction of astrocyte activation and reactive astrogliosis in mouse brain following maternal exposure to carbon black nanoparticle. *Part. Fibre Toxicol.* 14, 4.
- Phuyal, S., Kaseem, M., Rubio, L., Karlsson, H.L., Marcos, R., Skaug, V., Zienolddiny, S., 2017. Effects on human bronchial epithelial cells following low-dose chronic exposure to nanomaterials: a 6-month transformation study. *Toxicol. In Vitro* 44, 230–240.
- Rowe, L.A., Degtyareva, N., Doetsch, P.W., 2008. DNA damage-induced reactive oxygen species (ROS) stress response in *Saccharomyces cerevisiae*. *Free Radic. Biol. Med.* 45, 1167–1177.
- Simon, H.U., Haj-Yehia, A., Levi-Schaffer, F., 2000. Role of reactive oxygen species (ROS) in apoptosis induction. *Apoptosis* 5, 415–418.
- Stone, K.C., Mercer, R.R., Gehr, P., Stockstill, B., Crapo, J.D., 1992. Allometric relationships of cell numbers and size in the mammalian lung. *Am. J. Respir. Cell Mol. Biol.* 6, 235–243.
- Suarez-Fernandez, M.B., Soldado, A.B., Sanz-Medel, A., Vega, J.A., Novelli, A., Fernandez-Sanchez, M.T., 1999. Aluminum-induced degeneration of astrocytes occurs via apoptosis and results in neuronal death. *Brain Res.* 835, 125–136.
- Svensson, I., Artursson, E., Leanderson, P., Berglund, R., Lindgren, F., 1997. Toxicity in vitro of some silicon carbides and silicon nitrides: whiskers and powders. *Am. J. Ind. Med.* 31, 335–343.
- Vaughan, G.L., Trently, S.A., Wilson, R.B., 1993. Pulmonary response, in vivo, to silicon carbide whiskers. *Environ. Res.* 63, 191–201.
- Wu, J., Wang, C., Sun, J., Xue, Y., 2011. Neurotoxicity of silica nanoparticles: brain localization and dopaminergic neurons damage pathways. *ACS Nano* 5, 4476–4489.
- Yang, X., He, C., Li, J., Chen, H., Ma, Q., Sui, X., Tian, S., Ying, M., Zhang, Q., Luo, Y., Zhuang, Z., Liu, J., 2014. Uptake of silica nanoparticles: neurotoxicity and Alzheimer-like pathology in human SK-N-SH and mouse neuro2a neuroblastoma cells. *Toxicol. Lett.* 229, 240–249.
- Zhou, M., Xie, L.L., Fang, C.J., Yang, H., Wang, Y.J., Zhen, X.Y., Yan, C.H., Wang, Y.J., Zhao, M., Peng, S.Q., 2016. Implications for blood-brain-barrier permeability: in vitro oxidative stress and neurotoxicity potential induced by mesoporous silica nanoparticles: effects of surface modification. *Rsc Adv.* 6, 2800–2809.